

# NEMS Mass Sensor by Focused Ion Beam Fabrication

B. Boonliang\*, P. D. Prewett, M. C. L. Ward and P. T. Docker

The University of Birmingham, Research Centre for Micro-Engineering and Nanotechnology,  
Birmingham, B15 2TT, UK, \*[BXB915@bham.ac.uk](mailto:BXB915@bham.ac.uk)

## ABSTRACT

The possibility of using paddle-type resonators for mass/chemical sensor applications is explored. An analytical model of a magneto-motive-driven paddle resonator is derived to determine intrinsic behaviour, response and sensitivity to mass adsorption. Confirmation of the model was carried out using the ABAQUS FEA package. Preliminary devices have been manufactured using focused ion beam fabrication techniques.

**Keywords:** FIB fabrication, mass sensor, nano-resonator

## 1 INTRODUCTION

At present, chemical detection technologies are principally based on adaptation of laboratory techniques. A number of spectroscopic methods that utilise optical absorption, light scattering, luminescence, atomic fluorescence or refractive index changes have been explored [1]. However, these methods are still based on laboratory analysis on extracted samples. Hence they do not provide real-time data and are generally complicated, time-consuming and expensive.

Recently, there has been a rising demand for real-time in situ chemical detection technologies, as monitoring of specific substances is vital in many industrial and research fields, ranging from clinical analysis, environmental control to industrial processes. The demands also extend to safety and military services, especially for hazardous materials, contraband and explosive chemicals.

Interest in sensors and actuators and the rapid growth of nanotechnology have led to a new horizon for the development of sensor devices. The availability of new fabrication technologies is promoting the growth of micro- and nano-electromechanical systems (MEMS and NEMS), oscillators and resonant systems.

Many researchers have shown that microcantilevers (MC) in dynamic mode are a major candidate for such a task [2, 3], providing exceptionally high sensitivity to additional mass [4].

This paper explores another type of resonator, namely a paddle resonator, which operates in dynamic mode through torsional vibration of its shafts. It offers better response to changes in additional mass with structures of similar size to MC. Focused Ion Beam (FIB) is the selected manufacturing technique. It is an extremely versatile

fabrication tool which has the capabilities for milling, deposition and inspection in nanometer-scale.

## 2 DESIGN PRINCIPLES

### 2.1 Structural Design

Essentially, a paddle resonator is a double-clamped beam with large plate at the mid-point. It is designed to resonate at fundamental frequency in torsion through the beams. The plate is to be coated by chemically selective polymer compounds for detection. The schematic drawing of the structure is shown in Fig 1. This structure exhibits many possible advantages over MC, such as;

- Larger area of detection with similar sized structure
- Linear response to mass addition
- Less intrinsic bending in the beams due to the weight of the detecting plate
- No stress induced effect, upon detection, as beams do not have chemical layer coating
- Utilise bending moment to drive, therefore less power required for significant movement

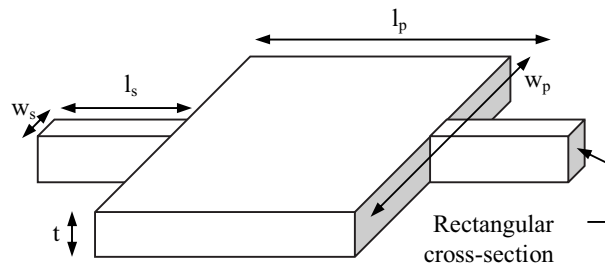


Fig. 1. Schematic drawing of the paddle resonator

From Fig. 1,  $l_p$  and  $w_p$  are length and width of the plate,  $l_s$  and  $w_s$  are length and width of the shaft and  $t$  is thickness of membrane.

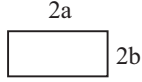
The movement in the beams can be described by the torque-deflection equation:

$$T = GJ_t \frac{\partial \theta}{\partial x} \quad (1)$$

Where  $T$  is torque,  $G$  is shear modulus,  $\theta$  is angle of twist and  $x$  is distance along the beam.  $J_t$  is the “Torsional Parameter” of a non-circular bar which is defined below [5].

$$J_t = ab^3 \left[ \frac{16}{3} - 3.36 \frac{b}{a} \left( 1 - \frac{b^4}{12a^4} \right) \right] \quad (2)$$

(for rectangular cross-sectional beam of  $a \geq b$ )



By considering a uniform shaft segment of length  $l_s$ , with overall angular deformation  $\theta$ , the torsional stiffness,  $K_t$ , may be written as:

$$K_t = \frac{T}{\theta} = \frac{GJ_t}{l_s} \quad (3)$$

The mass of the plate  $m_p$  generates rotational resistance or “Polar Mass Moment Of Inertia”  $J_p$ , given by:

$$J_p = \frac{m_p}{12} (w_p^2 + t^2) \quad (4)$$

During vibration, it is assumed that the plate is a rigid structure rotating about the weightless shafts. The natural frequency  $f_n$  of the device is defined by:

$$f_n = \frac{1}{2\pi} \sqrt{\frac{2K_t}{J_p}} \quad (5)$$

## 2.2 Driving Force

The structure is to be driven at its natural frequency by the Lorentz force. The proposed layout of the drive-system is shown in Fig. 2. The tracks are to be FIB-deposited Platinum (Pt). The top track carries an AC current in the presence of perpendicular external magnetic field producing up-/downwards oscillating forces.

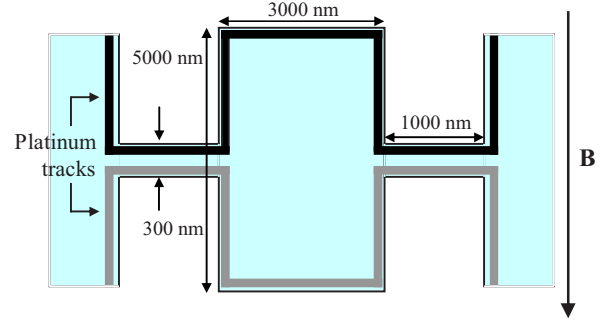


Fig. 2. Schematic drawing of paddle resonator and Pt tracks with dimensions

The top track of length  $l_{pt}$ , carrying current  $I$  in magnetic field  $B$ , generates torque  $T$  producing a twisting angle  $\theta$ , which can be described by the equation below.

$$T = \frac{GJ_t \theta}{l_s} = Fd \quad (6)$$

Where  $d$  is half the width of the plate and  $F$  is Lorentz force which is;

$$F = BIl_{pt} \quad (7)$$

By rearranging the Equation (7) and assuming a  $Q$  factor, the angle of twist (maximum amplitude) can be written, in terms of all factors, as:

$$\theta = \frac{QBIl_{pt}l_s d}{2GJ_t} \quad (8)$$

## 2.3 Pick-Up System

Monitoring change in natural frequency can be done through exploitation of electromagnetic induction.

The Faraday-Lenz law of Electromagnetic Induction states that:

$$\varepsilon = - \frac{d\Phi_b}{dt} \quad (9)$$

Where  $\varepsilon$  is induced emf and  $\Phi_B$  is magnetic flux through a finite area. During resonance, the non-current-carrying bottom track in Fig. 2.2 cut magnetic field line perpendicularly, generating an emf of:

$$\varepsilon = -B l_{pt} r \frac{d\theta}{dt} \quad (10)$$

By assuming the excitation to be simple harmonic with  $\theta = \theta_{\max} \sin pt$  and  $p = 2\pi f$ . Equation (10) can be rewritten to get the final form of  $\varepsilon$ ;

$$\varepsilon = -B l r \theta_{\max} p \cos pt \quad (11)$$

The induced emf is to be monitored through a controlled feedback loop, which will readjust the driving frequency automatically upon the detection of a shift in natural frequency. Thus the shift can be recorded then converted to additional mass through calculation.

### 3 FABRICATION

The resonant device is made from 200 nm-thick  $\text{Si}_3\text{N}_4$  membrane window supplied by Silson Ltd. All fabrication is done using the FEI Strata™ DB 235. The process has 4 steps involving both Pt deposition and  $\text{Si}_3\text{N}_4$  millings.

The SEM images of the device, Fig. 3, show a FIB-fabricated paddle resonator. The Pt tracks are the smallest feature, roughly 75 nm in width and 75 nm in height. The process also exhibits good reproducibility and multiple-device-manufacturing capability.

A smaller resonator, fabricated from 100 nm-thick  $\text{Si}_3\text{N}_4$  membrane window to further show the capability of the FIB, is shown in Fig. 4, with a plate dimension of 1000 nm x 1000 nm and 400 nm-long beams.

### 4 ANALYSIS AND RESULTS

By analytically modelling the theoretical behaviour of the device with the dimensions (as in Fig. 2), the natural frequency of the  $\text{Si}_3\text{N}_4$  paddle (i.e. without the Pt tracks) is predicted to be approximately 10.6 MHz. The ABAQUS Finite Element Analysis package confirms that the device will be in torsional vibration at fundamental frequency of 12.5 MHz. This indicates a reasonable correlation between the analytical model and the FEA methods. The difference of 2 MHz is believed to be explained by stress in the structure upon rotation in the shafts, which the FEA package took into account. With the addition of Pt tracks, the analytical model predicts that the natural frequency would drop down to about 8.8 MHz, compared to the FEA prediction of 11.5 MHz.

Hence, the analytical model is believed to be sufficient enough to preliminarily indicate more complex behaviours of the device i.e. with proposed drive and pick up systems.

The model prediction of the device's response to mass adsorption is shown in Fig. 5. Sensitivity is approximately 300 Hz per femtogram. This is based on the assumptions of  $B$  of 1 T, input  $I$  of 100  $\mu\text{A}$  and  $Q$  of 10000. This produce roughly  $10^\circ$  angle of twist which results an induced emf of roughly 70  $\mu\text{V}$  peak-to-peak.

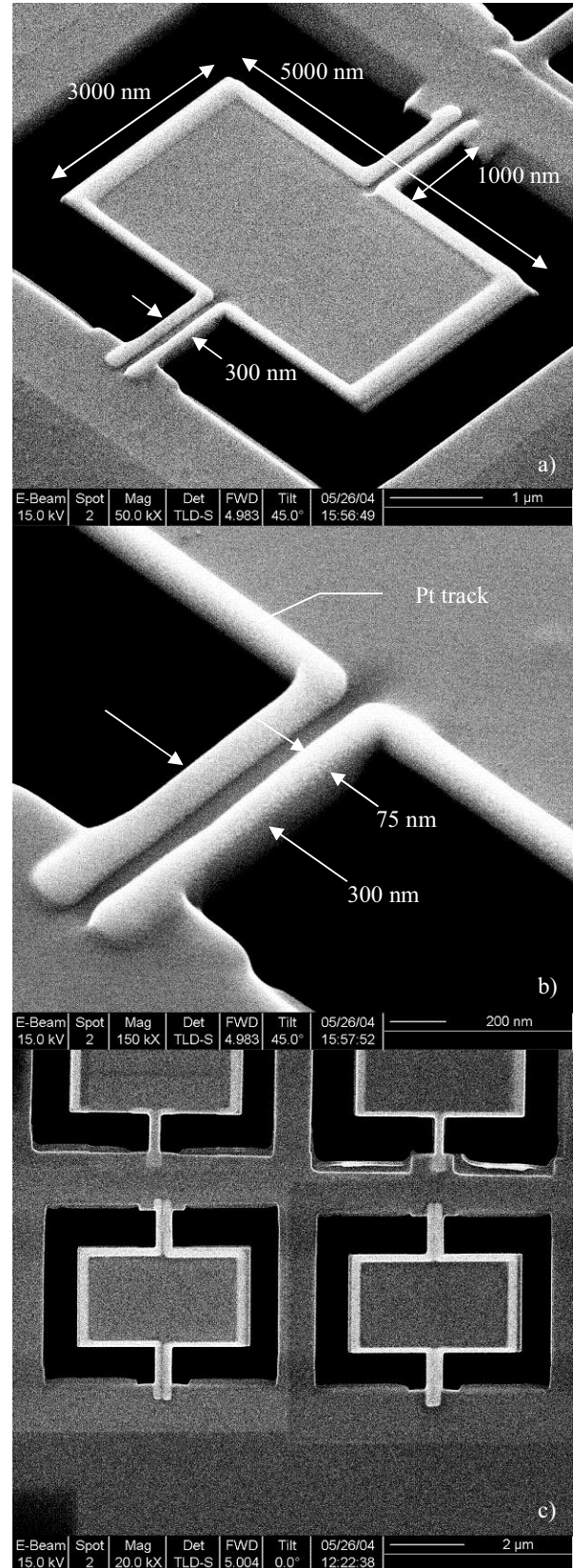


Fig. 3. a) Whole device, b) Close-up of shaft and tracks, c) 2 resonators made in one process

By applying the same analytical model to the device in Fig. 4, the smaller paddle resonator would have natural frequency of 79.9 MHz, with mass sensitivity of 133 Hz per attogram.

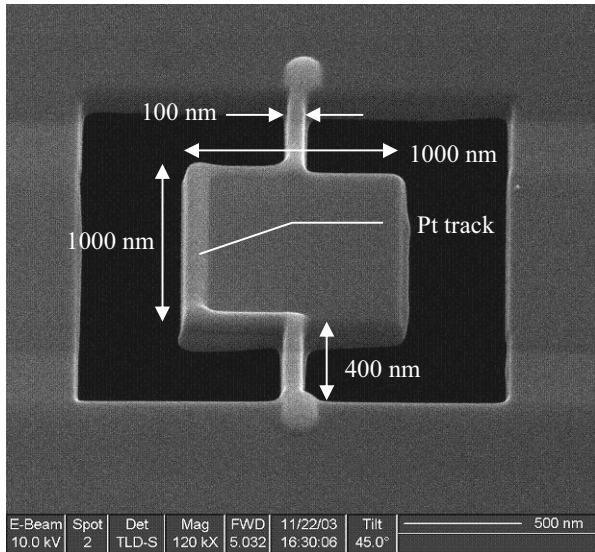


Fig. 4. Submicron FIB fabricated paddle with Pt track

### Shift in Natural Frequency - Adsorption Mass

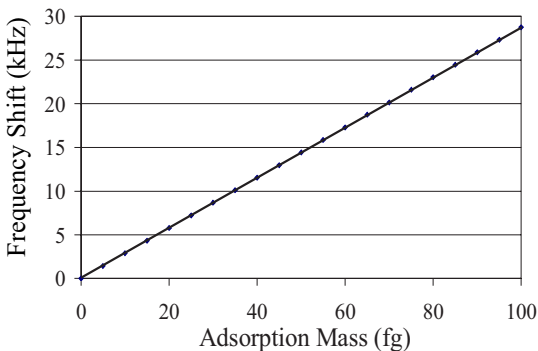


Fig. 5. Plots of frequency shift upon mass adsorption showing a linear response of the resonator to mass addition

### CONCLUSION

Analysis of a simple paddle resonator using analytical and FEA modeling show acceptable agreement. The device, driven to resonance by Lorentz forces and with manageable electromagnetic induction readout, shows high sensitivity to mass adsorption with linear response. FIB milling and deposition have been used successfully to fabricate initial experimental devices in  $\text{Si}_3\text{N}_4$  membranes, with good integrity and reproducibility. The capability of FIB for fabrication of submicron (NEMS) prototype has been demonstrated.

### REFERENCES

- [1] P. G. Datskos, M. J. Sepaniak, C. A. Tipple and N. Lavrik, *Sensors and Actuators B* 76, 393-402, 2001
- [2] J. Mertens, E. Finot, T. Thundat, A. Fabre, M. H. Nadal, V. Eyraud and E. Bourillot, *Ultramicroscopy* 97 (1-4), 119-126, 2003
- [3] A. Passian, G. Muralidharan, A. Mehta, H. Simpson, T. L. Ferrell and T. Thundat, *Ultramicroscopy* 97 (1-4) 391-399, 2003
- [4] B. Ilic, H. G. Craighead, S. Krylov, W. Senaratne, C. Ober and P. Neuzil, *Journal of Applied Physics*, Vol. 95, 3694-3703, 2004
- [5] R. J. Roark, "Roark's formulas for stress and strain". 6<sup>th</sup> Edition, McGraw-Hill, 1996